Bull Astr Soc India (1990) 18, 149-165

Radiation transfer in fast moving fluids

A. Peraiah
Indian Institute of Astrophysics, Bangalore 560 034

1. Introduction

Most of the information from stars, galaxies, nebulae comes through the study of their spectra. The information we obtain from spectra concerns the geometrical shape, chemical abundances, thermodynamical properties of the medium, dynamics of the medium, etc. This information will lead to the study of stellar evaluation.

Spectral lines can be studied at various levels: for example, one can use a logarithmic table or a small, inexpensive pocket calculator to obtain simple physics, by employing Doppler profile function which is nothing but an exponential function. However, if we introduce slightly complicated physics by only one step further such as increasing the number of absorbing or emitting ions, we have to use a fairly good computer and the problem can be made increasingly complicated by including more and more realistic physics. If one would like to compute the spectral lines as realistically as possible one requires to perform complicated calculations on a supercomputer.

There are several physical aspects that one should consider in computing the spectral lines. In the following we describe various factors influencing the formation of spectral lines.

2. Broadening mechanisms

There are several types of broadening, namely natural, thermal, collisional, radiation, Zeeman, Stark, Doppler, Compton broadening, etc. If stellar atmosphere contains free electrons then we have to consider the Compton broadening along with Doppler broadening which remains an outstanding problem yet to be attempted. All the broadening mechanisms are operating in the stellar atmospheres and they influence formation of spectral lines.

3. Photon or partial frequency redistribution

Photons have certain probabilities of getting emitted at different frequencies and directions after scattering. This again depends upon the type of broadening. For example the upper level or lower level or both, can be subjected to collisional broadening or radiation broadening or any other broadening and/or a combination of any of these broadening mechanisms. If one likes to calculate the spectral lines by including such broadening mechanisms, it requires considerable amount of effort on the part of worker.

4. Chemical species

The line strengths depend upon the number of absorbing or the number of emitting atoms of a particular element. This again depends on how many neutral or excited atoms exist for the formation of particular given line. This in turn depends upon the temperature, geometrical structure, pressures, electron density, velocity fields of the media, and so forth Further, the distribution of a particular element across the medium is more important for the formation of line and we can derive this distribution only from the strength of the line that we observe after a detailed calculation of the formation of the line. There may not be an equilibrium between emission and absorption profiles. This leads up to a study of non-equilibrium thermodynamic properties of the atmosphere. We have to take this into account and we have to calculate the number of atoms in various stages of ionization, excitation, using the non-local thermodynamic equilibrium. When one uses this type of physics the probability that a photon is thermalized becomes extremely small, in which case scattering plays a dominant role in the formation of lines. This renders the calculation more difficult because one has to estimate the interaction of frequency and angle. This aspect alone would force us to develop new techniques for obtaining solutions of line transfer.

5. Geometry and dynamical aspects

Normally when we consider the early type stars we assume that the thickness of atmosphere is small compared to the radius of the star. However, in the case of supergiant stars the atmospheres are several times the radius of the star. When a photon leaves the centre of the star it takes considerable amount of time to reach the surface, and therefore it is important to study the physical changes that the photon has undergone during this time while travelling across the medium. It becomes necessary to solve the equation of transfer in a spherically symmetric and geometrically extended atmosphere.

5.1. *Plane parallel and spherical symmetry*

In plane parallel situation the radius of the star is assumed to be small. In extended stellar atmospheres, this approximation fails. Therefore, we have to consider the spherically symmetric case. This can be understood from the figures 1 and 2.

In figure 1, we have depicted a plane parallel stratification in which the layer is extremely small compared to the radius of the star and the axis of symmetry is along the direction of the radius. The ray makes a constant angle with the axis of symmetry or the radius vector. In figure 2, the angle made by the ray with the radius vectors changes continuously. This can be understood from the equation of transfer

$$\mu \frac{\partial I}{\partial r} + \frac{1-\mu^2}{r} \frac{\partial I}{\partial \mu} = K(S - I), \qquad \ldots(1)$$

where μ is the cosine of the angle made by the ray with the radius vector r; I the specific intensity of the ray; K the absorption coefficient; and S the source function. We notice that the second term on the left side describes variation of specific intensity with respect to μ. We also notice that the quantity $1/r \to 0$ as $r \to \infty$, and we recover the plane parallel approximation.

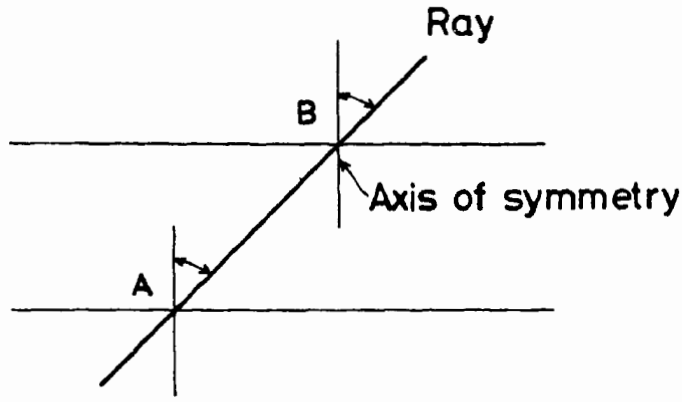

Figure 1. Plane parallel geometry

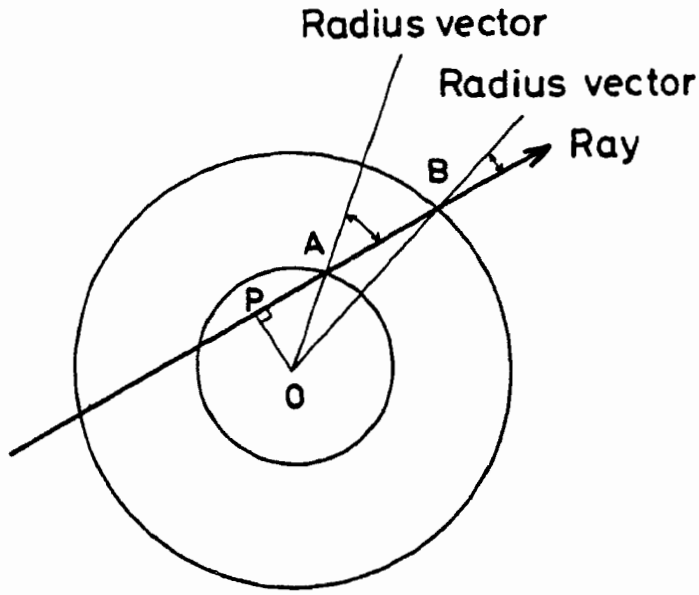

Figure 2. Spherically symmetric geometry.

The observations of many spectral lines show that the medium is not stationary but in motion. This means that we have to consider the hydrodynamic aspect of the medium and introduction of these aspects into the calculation requires special efforts.

One of the natural ways of calculating the lines in a moving medium is to employ what is called the rest frame. In this, frame, one computes the spectral lines and observes the emission or absorption of the photon by a moving medium at a point which is at rest with respect to the centre of the star.

5.2. *Rest frame*

We have calculated lines in the rest frame function R_{I} and R_{II}. The transfer equation is

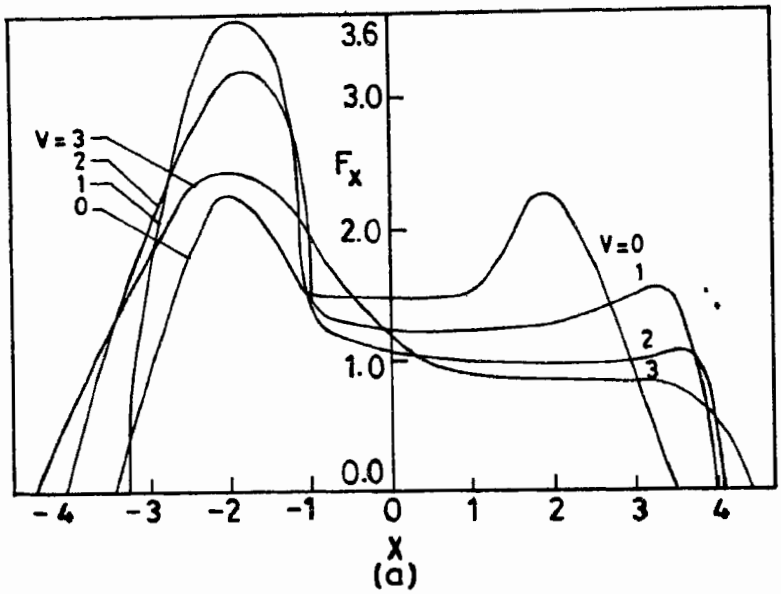

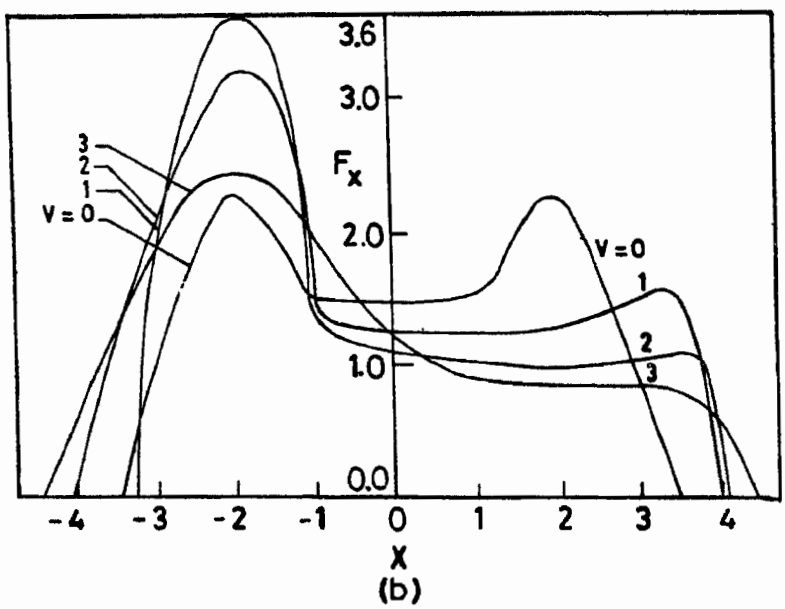

Figure 3. Integrated profiles for R_1 . $\epsilon = 10^{-4}$, $\beta = 0$.
(a) $B/A = 2$, (b) $B/A = 10$. ϵ is the probability of thermalization of photons by collisional de-excitation and β is the ratio of continuum to line absorption and B/A is the ratio of outer to inner radii of the spherical shell. R_1 is the redistribution function.

given by (see Wehrse & Peraiah 1979)

$$\mu \frac{\partial I(x, \mu, r)}{\partial r} + \frac{1-\mu^2}{r} \frac{\partial I(x, \mu, r)}{\partial \mu} + \chi(x, r)\,[I(x, \mu, r)]$$

$$= \chi(x, r)\left\{\int_{-\infty}^{+\infty} dx' \int_{-1}^{+1} R(x, x')\, I(x', \mu')\, d\mu' + \Phi(x)\, S(r)\right\}, \quad \ldots(2)$$

$$R_{\text{II-A}}(x, x') = \int_{|x-x'|/2}^{\infty} e^{-u^2}\left[\tan^{-1}\left(\frac{\underline{x}+u}{a}\right) - \tan^{-1}\left(\frac{\bar{x}-u}{a}\right)\right] du. \quad \ldots(3)$$

Here $\underline{x}$ and $\bar{x}$ are the minimum and maximum of x, x'; $I(x, \mu, r)$ is the specific intensity making an angle $\cos^{-1}\mu$ with the radius vector r; $\chi(x, r)$ is the absorption coefficient; $\Phi(x)$ the profile function; and $R(x, x')$ the redistribution function.

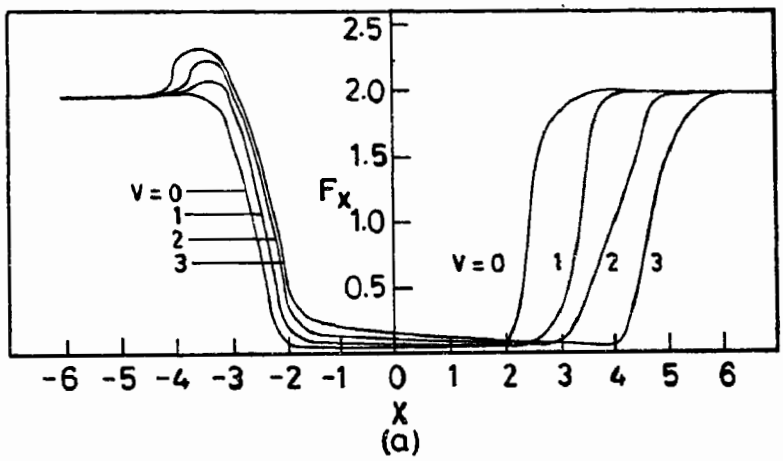

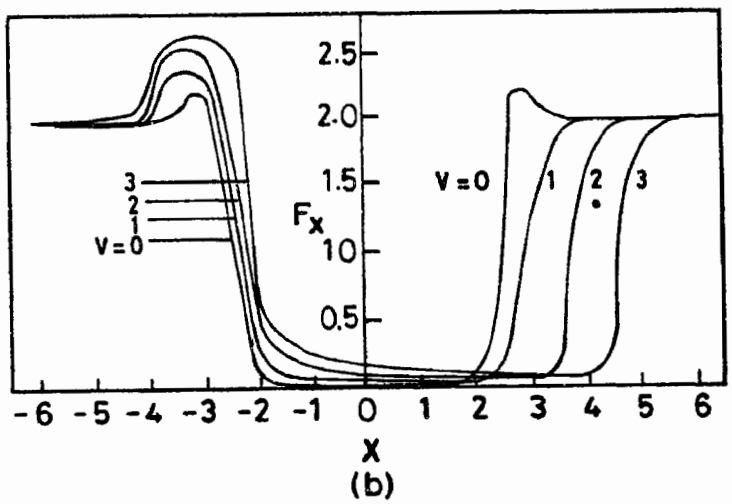

Figure 4. Integrated profiles for $R_1 . \epsilon = \beta = 0$. (a) $B/A = 2$, (b) $B/A = 10$.

$$x = \frac{\nu - \nu_0}{\Delta_D}, \; x' = \frac{\nu' - \nu_0}{\Delta_D}, \; \Delta_D = \text{Doppler width} \qquad \ldots(4)$$

and the angle independent R_I given is by

$$R_{I\text{-}A}(x, x') = \frac{1}{2} \operatorname{erfc}(|\bar{x}|), \qquad \ldots(5)$$

$$\operatorname{erfc}(x) = \frac{2}{\sqrt{\pi}} \int_{-\infty}^{+\infty} e^{-t^2} \, dt \qquad \ldots(6)$$

However, this approach has a major drawback. Because of the dependence of the absorption coefficient with angle and frequency due to Doppler shifts, we require to calculate the absorption coefficient whenever there is a change in the velocity; that is, changes in absorption coefficients must be incorporated in the angle-frequency mesh continuously along the radial grid. If the medium is moving with 100 Doppler widths, then we must have such a large grid which should incorporate -100 to $+100$ Doppler widths. Even if we employ the grid interval to be 1 Doppler width we require a 200 by 200 grid. This is only regarding the velocities of the medium. If we include angles and frequencies into the grid-size it becomes highly unmanageable. However, we need to study this kind of velocities whereas so far we were successful only up to one or two Doppler widths. If we employ large grids, the solution becomes unstable and incorrect.

5.3. *Comoving frame*

Therefore, in this connection we find the comoving frame to be the best way to simulate the spectral lines. In this frame we do not have the problem of dependence of absorption coefficient on velocity changes. Therefore the solution can be obtained with a small sized angle-frequency grid. The equation of transfer becomes (see Peraiah 1980)

$$\mu \frac{\partial I(x, \mu, r)}{\partial r} + \frac{1 - \mu^2}{r} \frac{\partial I(x, \mu, r)}{\partial \mu}$$

$$= K_L[\beta + \phi(x)] \, [S(x, r) - I(x, \mu, r)] + \left\{(1 - \mu^2) \frac{V(r)}{r}\right.$$

$$\left. + \mu^2 \frac{dV(r)}{dr}\right\} \frac{\partial I(x, \mu, r)}{\partial x}, \qquad \ldots(7)$$

where $V(r)$ is the radial velocity of the atmospheres measured in units of Doppler widths.

We were able to use this method to calculate the lines in a medium which is moving with as large as 100 Doppler widths (see figures 5-11). However at these high velocities, we have to take into account two important effects known as aberration and advection.

5.4. *Aberration and advection*

We are able to calculate the spectral lines formed in a medium which is moving at 100 Doppler widths or about 3000 to 4000 km s^{-1}. At these velocities what does happen to the medium and the radiation field? We shall have to estimate the real interaction of matter with radiation. At these velocities, the effects due to aberration and advection become

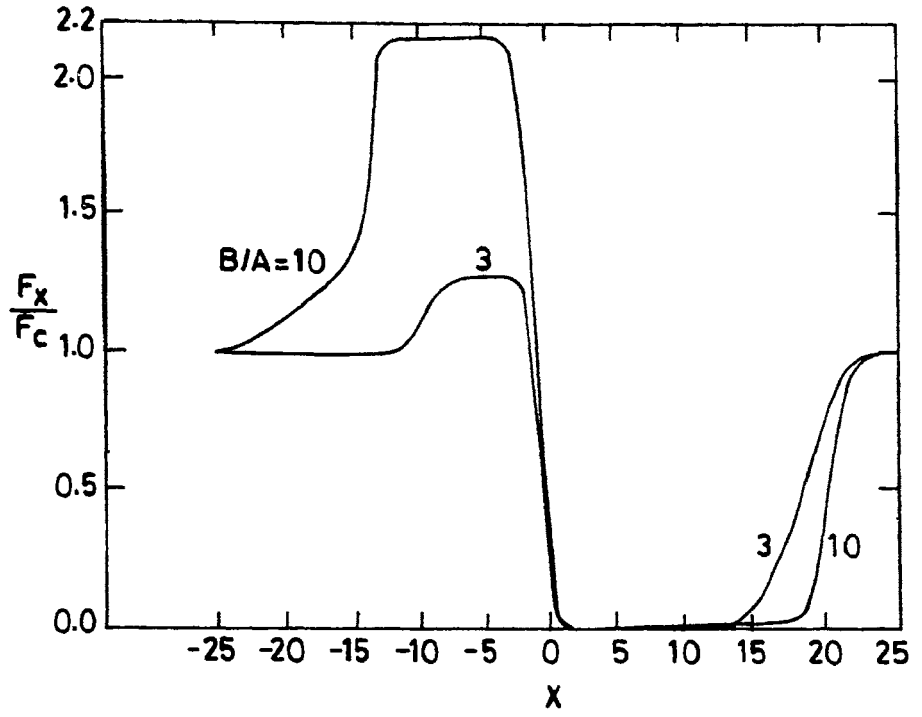

Figure 5. Flux profiles for different velocities of expansion.

prominent. Aberration is nothing but the delay in arrival of the photon from the moving object at the observer, while advection is a 'sweeping up of radiation' by the moving medium because of Doppler effects. How do these two phenomena change the radiation field?

Several years ago there were some calculations, which showed that the effects of aberration and advection in a medium moving with velocities small compared to the velocity of light are of the order of 6 to 7% in the spectral lines. However, it is difficult to understand how the medium which moves at such high velocities ($v/c = 0.01$ or 0.02) produces such small changes. Therefore, we have started working on these problems in a systematic way. The first thing that we did was to consider a simple model, that is calculate the effects in a plane parallel medium scattering monochromatic radiation coherently and isotropically. We found that the effects due to aberration and advection are considerable for the same type of the velocity other people have used. The differences in mean intensities are found to be of the order of 80% depending on the size of optical depth.

The equation of transfer with aberration and advection terms in plane parallel geometry is (Peraiah 1987)

$$(\mu + \beta)\frac{\partial I(z,\ \mu)}{\partial z} + \frac{\mu(\mu^2 - 1)}{c}\frac{\partial v}{\partial z}\frac{\partial I(z,\ \mu)}{\partial \mu} + \frac{3\mu^2}{c}\frac{\partial v}{\partial c} I(z,\ \mu)$$
$$= K[S - I(z,\ \mu)], \qquad \ldots(8)$$

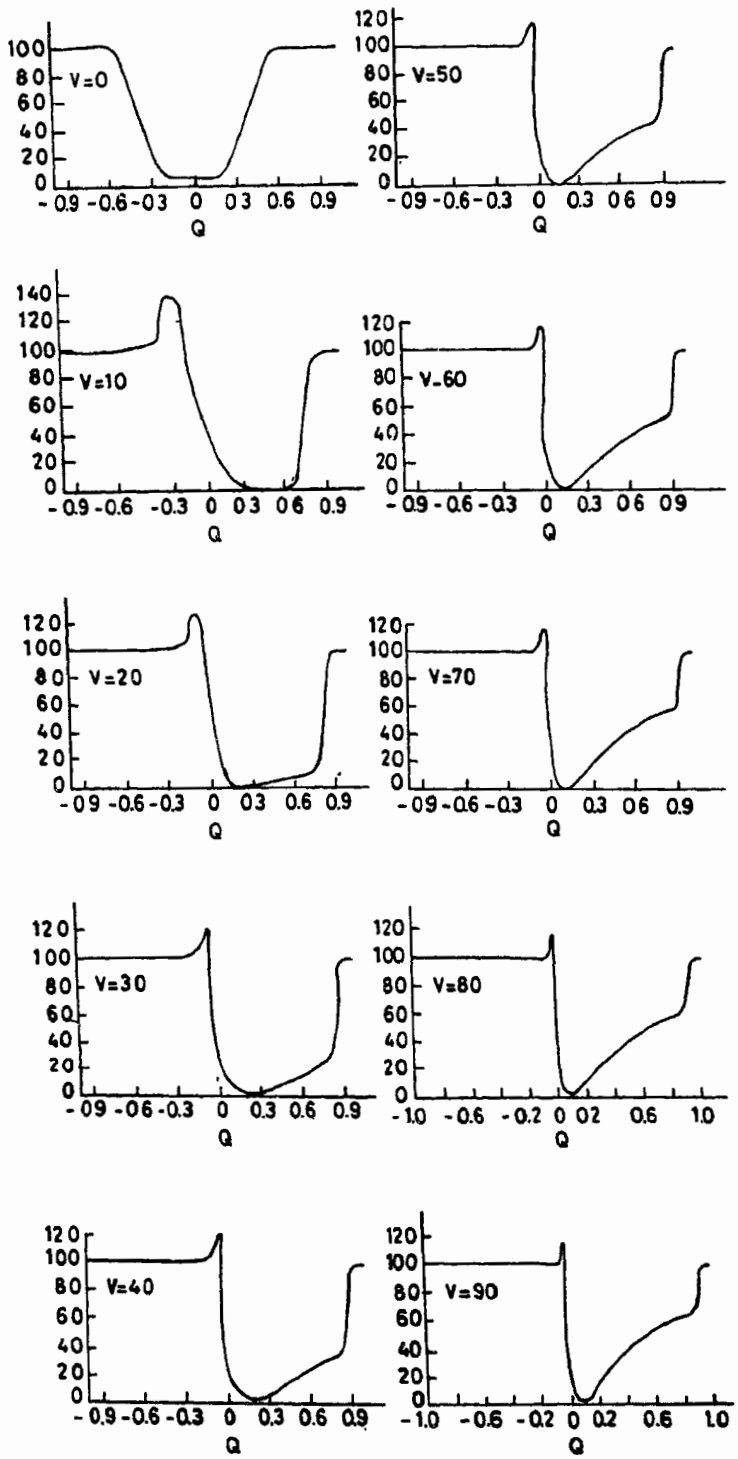

Figure 6. Flux profiles, for different velocities of expansion. V is in mean thermal units. $Q = X/X_{max}$.

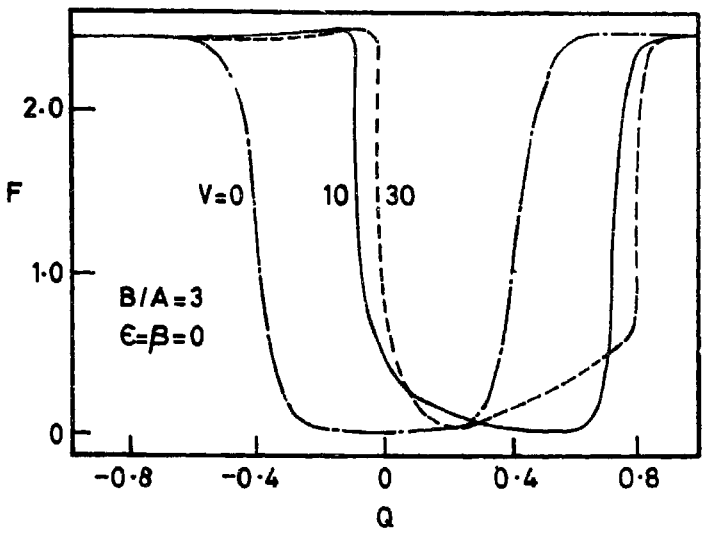

Figure 7. Flux profiles of the lines received at the observer and calculated with the redistribution function R_{I} in the comoving frame.

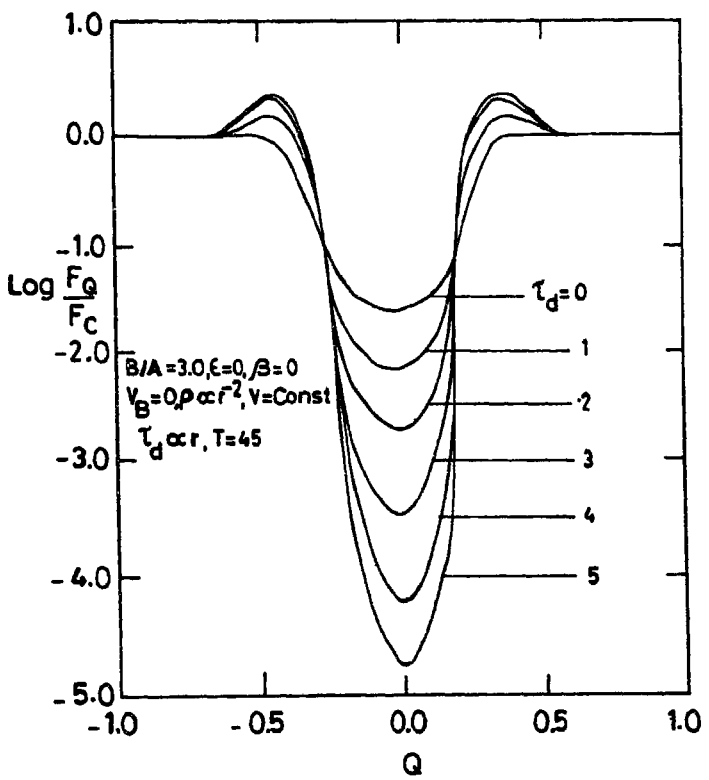

Figure 8. Line profiles formed in static medium in which dust changes proportionately with r and the gas density changes as r^{-2}. τ_d is the dust optical depth, T is the gas optical depth.

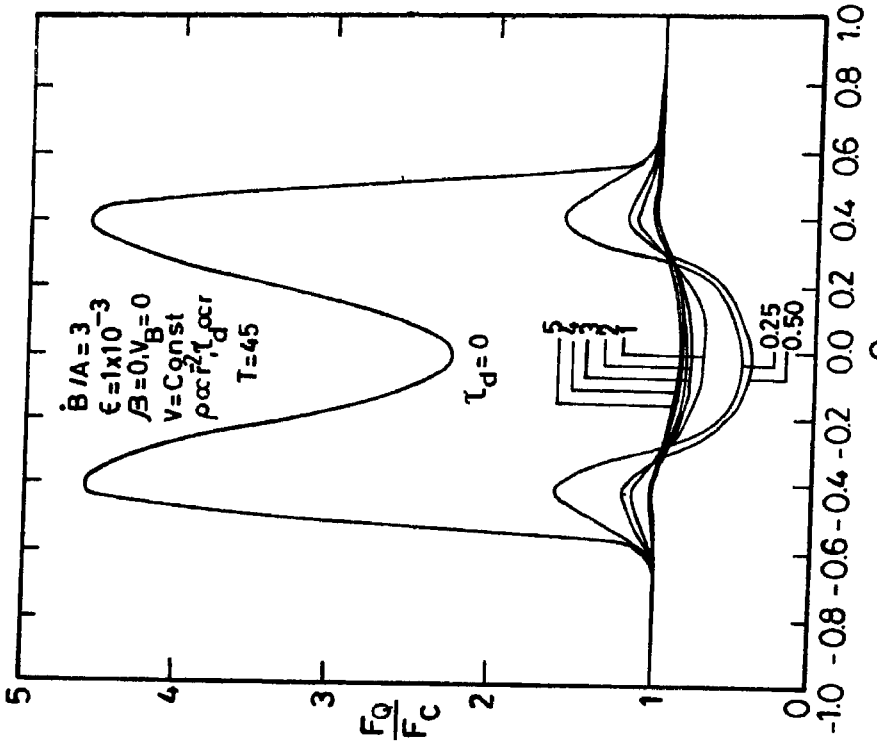

Figure 10. Line profiles formed in a static medium in which there is line emission and the dust is changing proportionately with r and gas density is changing as r^{-2}

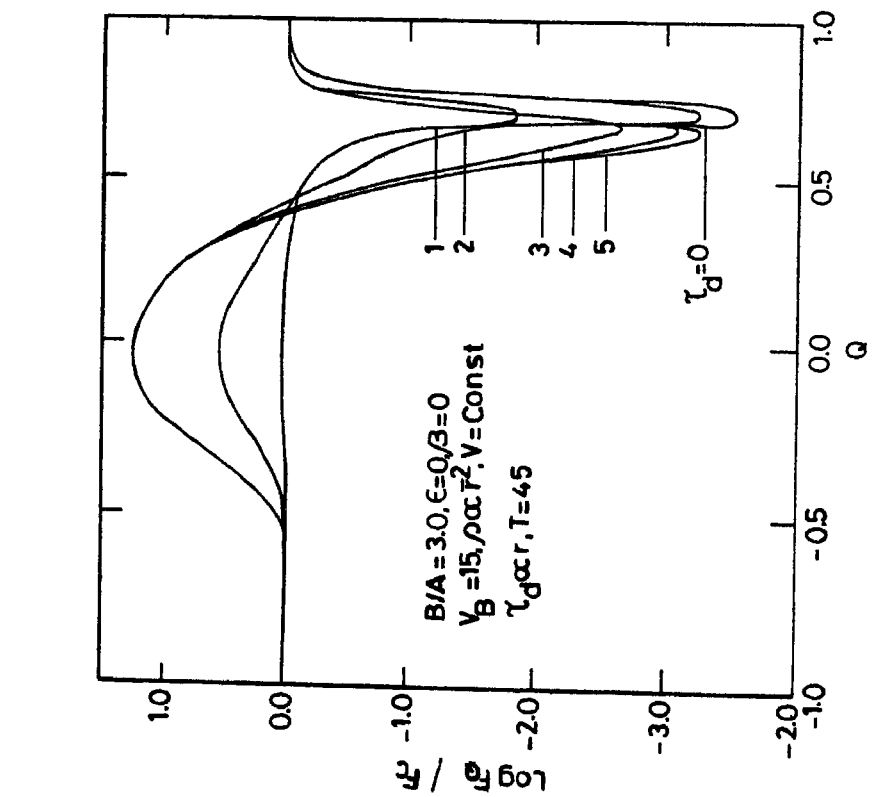

Figure 9. Same as those given in Figure 8 but with $V_B = 20$ Doppler units where V_B is the velocity at $r = B$.

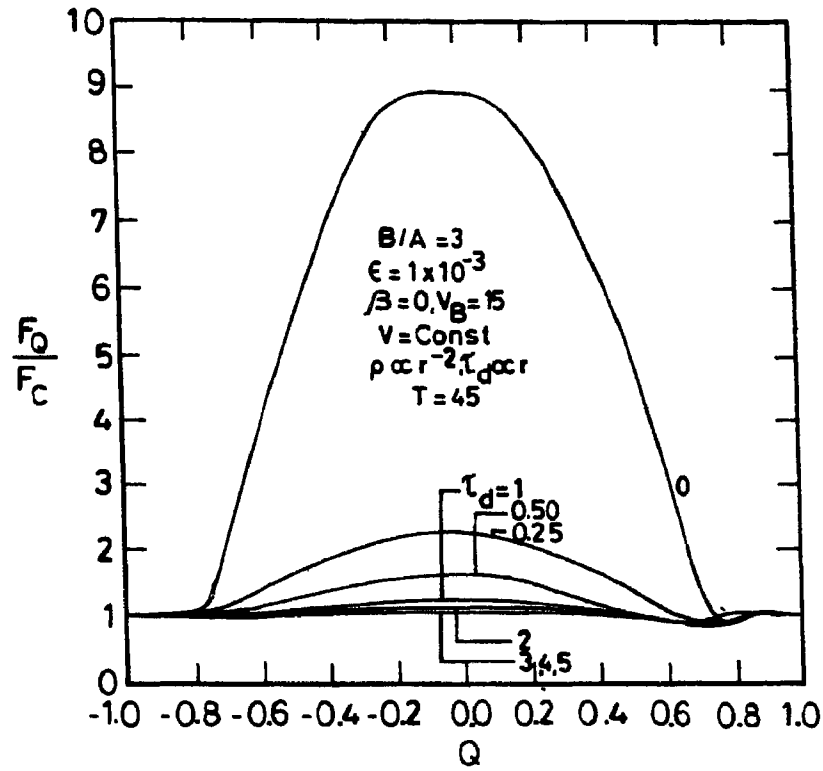

Figure 11. Same as those given in Figure 10 but with the expanding velocity $V_B = 20$ Doppler units.

where S is the source function given by

$$S = \frac{1}{2}\int_{-1}^{+1} P(z, \mu_1', \mu_2') I(z, \mu_2')\, d\mu_2'; \qquad \ldots(9)$$

and $P(z, \mu_1', \mu_2')$ is the isotropic phase function.

We shall make the substitution

$$\mu = \frac{\mu_0 - \beta}{\mu_0 + \mu_0 \beta}, \quad \beta = v/c,$$

μ_0 is the angle made by the ray with the axis of symmetry.

$$I = I_0 + \zeta I_z + \eta I_\mu + \zeta\eta I_{z\mu}, \qquad \ldots(10)$$

where

$$\zeta = \frac{z - \bar{z}}{\Delta z/2}, \quad \eta = \frac{\mu - \bar{\mu}}{\Delta \mu/2}, \qquad \ldots(11)$$

$$\bar{z} = \frac{1}{2}(z_1 + z_{i-1}), \quad \Delta z = (z_1 - z_{i-1}) \qquad \ldots(12)$$

$$\bar{\mu} = \frac{1}{2}(\mu_j + \mu_{j-1}), \quad \Delta\mu = (\mu_j - \mu_{j-1}) \qquad \ldots(13)$$

$$J = \frac{1}{2}\int_{+1}^{+1} I(\mu)\, d\mu. \qquad \ldots(14)$$

A velocity field produces Doppler shifts and aberration of photons and gives rise to advection terms which describes the sweeping up of the radiation by the moving fluid. The changes in the mean intensities are shown in figures 12 to 18.

We calculated the effects of aberration and advection on the line formation by using equation (15). The results are given in figures 19 and 20. We plotted the changes in the source functions. The changes warrant further study in this line.

$$(\mu_0 + \beta)\frac{\partial U(r, \mu_0, x)}{\partial r} + \frac{1-\mu_0^2}{r}\left\{(1 + \mu_0\beta(1 - \frac{r}{\beta}\frac{d\beta}{dr}\right\}\frac{\partial U(r, \mu_0, x)}{\partial \mu_0}$$
$$= \left\{\frac{v'}{r}(1-\mu_0^2) + \mu_0^2\frac{dv'}{dr}\right\}\frac{\partial U(r, \mu_0, x)}{\partial x}$$
$$\times\left[-3\left\{\frac{\beta}{r}(1-\mu_0^2) + \mu_0^2\frac{d\beta}{dr}\right\} + \frac{2(\mu_0+\beta)}{r}\right] U(r, \mu_0, x)$$
$$+ K(r)\{S(r, x) - U(r, \mu_0, x)\}. \qquad \ldots(15)$$

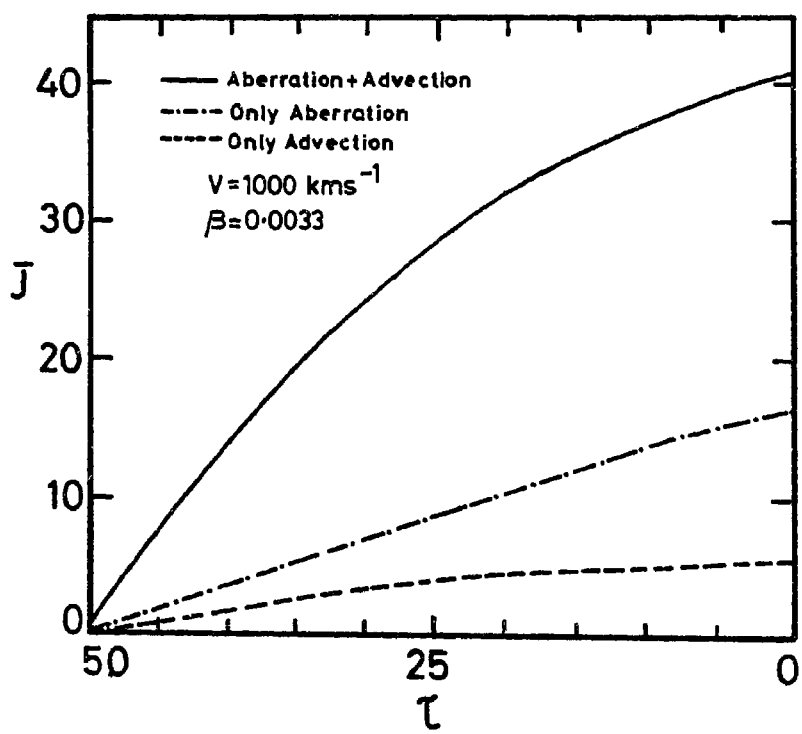

Figure 12. Values of $\bar{J}$ plotted separately for advection and aberration effects for $V = 1000$ km s^{-1} for $\tau_{max} = 50$, where $\bar{J} = (J(V>0) - J(V=0)/J(V=0) \times 100$.

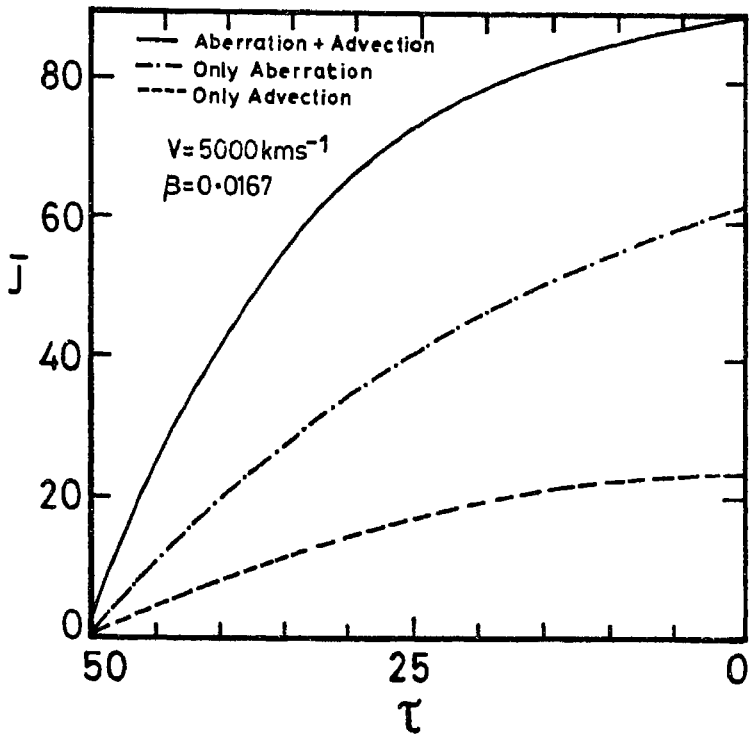

Figure 13. Same as those given in figure 12 with $V = 5000$ km s^{-1}

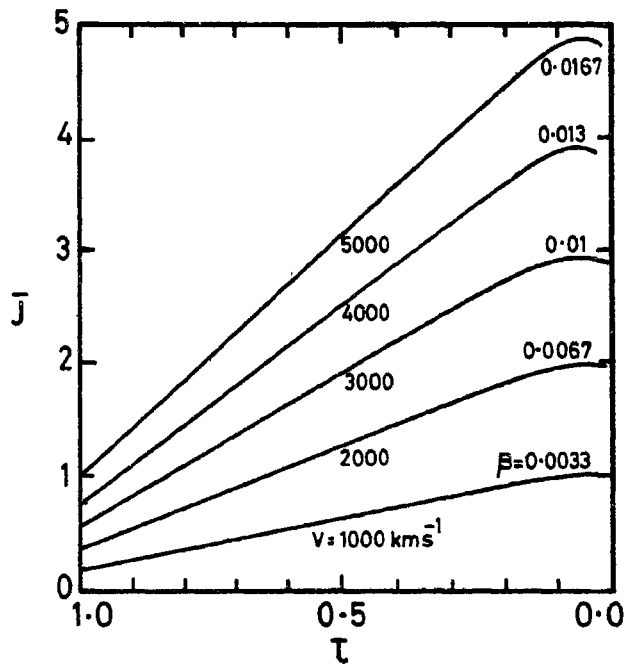

Figure 14. J plotted for $V = 1000$, 2000, 3000, 4000 and 5000 km s^{-1} for $\tau_{max} = 1$.

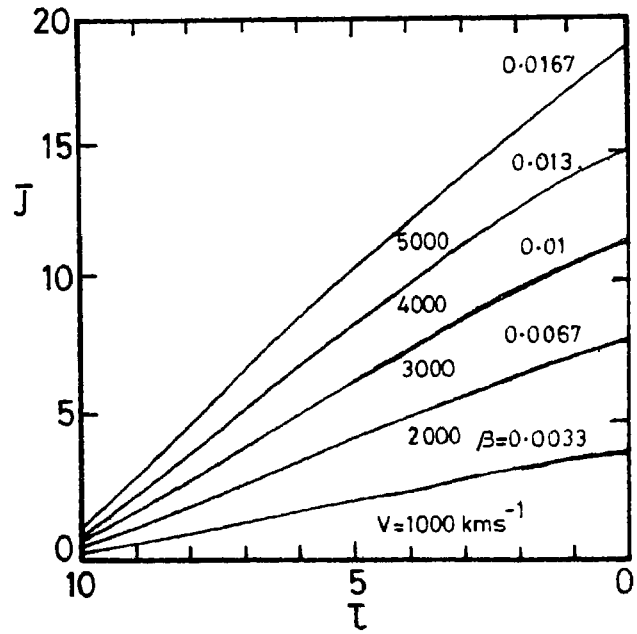

Figure 15. J plotted for $\tau_{max} = 10$

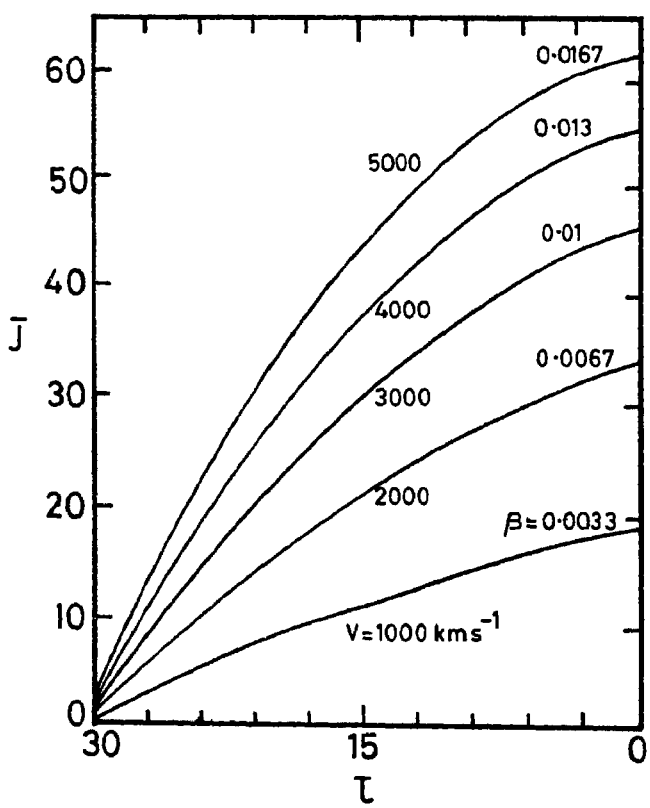

Figure 16. J plotted for $\tau_{max} = 30$.

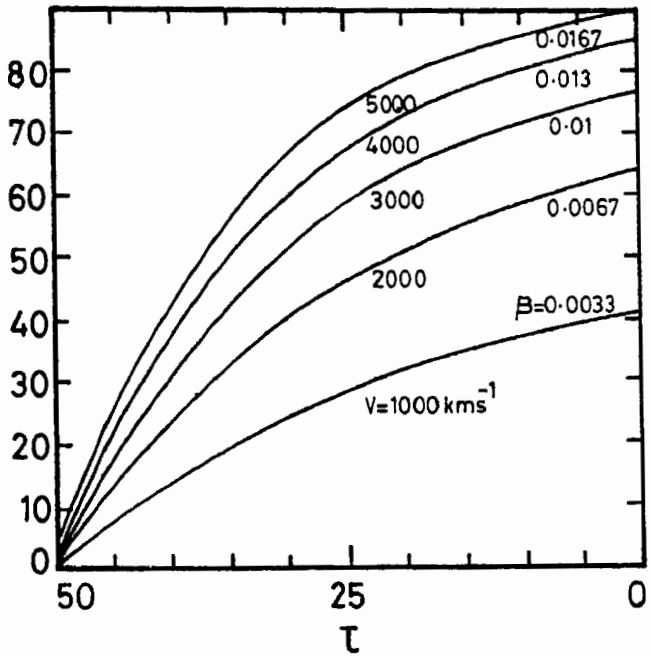

Figure 17. $\bar{J}$ plotted for $\tau_{max} = 50$.

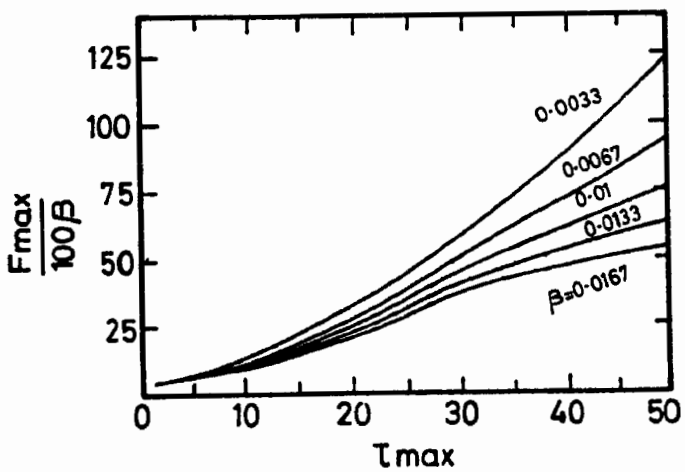

Figure 18. Amplification factor $J_{max}/100$ vs. τ_{max}.

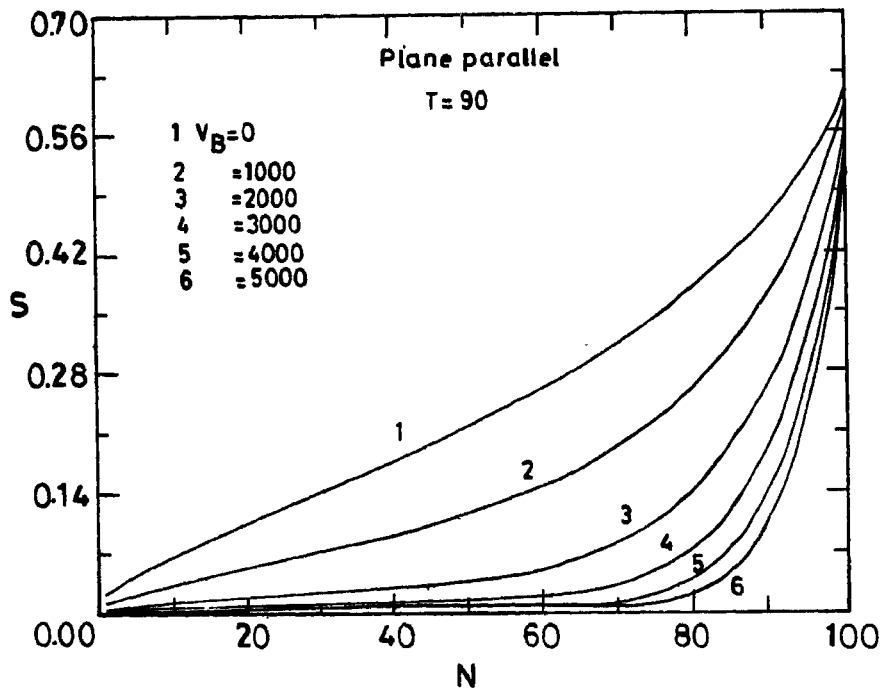

Figure 19. Line source functions $S_L = \int_{-1}^{+1} J(x, r)\phi(x)dx$ are plotted against shell numbers

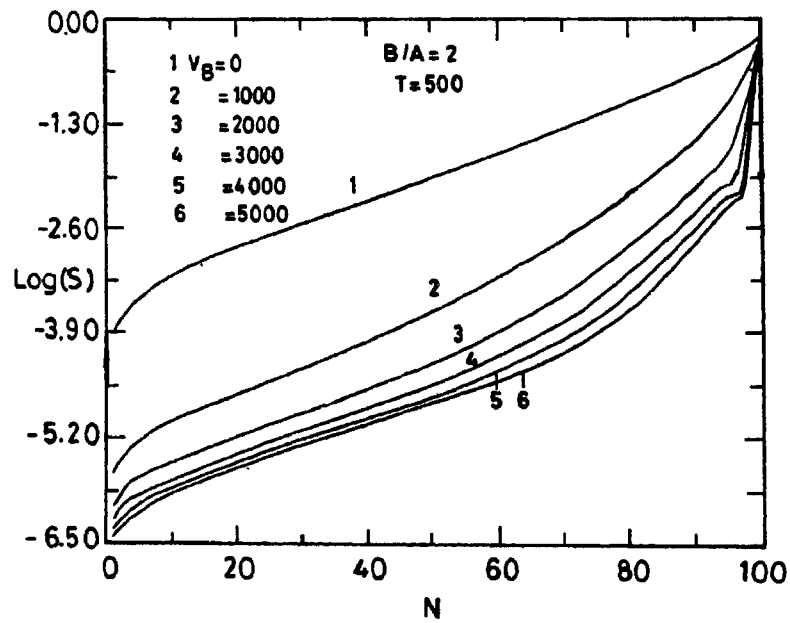

Figure 20. Same as given in figure 19 with $B/A = 2$ and $T = 500$.

References

Peraiah, A. (1979) *Ap. Sp. Sci.* **63**, 267
Peraiah, A. (1980) *Kodaikanal Obs. Bull Ser A.* **3**, 17.
Peraiah, A. (1980, 1987) *J. Ap. Astr.* **1**, 3; *Ap. J.* **317**, 271
Peraiah, A. (1989) to be published
Paraiah, A., Varghese, B. A & Srinivasa Rao, M (1987) *Astr Ap. Suppl.* **69**, 345
Wehrse, R. & Peraiah, A. (1979) *Astr. Ap.* **71**, 289.

Discussion

Vardya : Under what conditions is the difference between ϕ_{ab} and ϕ_{em} large?
Peraiah : When complete redistribution in the line is employed we do not find ϕ_{em} different from ϕ_{ab}. However when we employ partial frequency redistribution R_I, R_{II}, R_{III} etc., we notice that ϕ_{em} is very much different from ϕ_{ab}, sometimes by orders of magnitude. This is essentially saying that ϕ_{em} and ϕ_{ab} depend on the type of broadening mechanism we employ, *e.g.* R_I, R_{II}, R_{III} etc.
Vardya : Have you used this analysis on SN 1987 A?
Peraiah : No. We are trying to apply this method to SN 1987A.
Vardya : In a lighter vein how did you check the numbers in such a thick output?
Peraiah : By hope and perseverance.
Chandra : In physical systems we have multilevel system. Have you applied this approach to multilevel system or not?
Peraiah . Yes. We have calculated Ca II H & K (3968 Å, 3933 Å) and infrared triplet lines 8498 Å, 8662 Å, 8542 Å in a slowly expanding medium. See Rangarajan, Mohan Rao & Peraiah (1981) *Kodaikanal Obs. Bull. Ser. A* **3**, 75.